PHILOSOPHICAL TRANSACTIONS B

royalsocietypublishing.org/journal/rstb

Research

Cite this article: Fu Z *et al*. 2020 Sensitivity of gross primary productivity to climatic drivers during the summer drought of 2018 in Europe. *Phil. Trans. R. Soc. B* **375**: 20190747.
http://dx.doi.org/10.1098/rstb.2019.0747

Accepted: 14 June 2020

One contribution of 16 to a theme issue 'Impacts of the 2018 severe drought and heatwave in Europe: from site to continental scale'.

Subject Areas:
ecology, environmental science

Keywords:
drought, gross primary productivity, sensitivity, Europe, eddy covariance, soil moisture

Author for correspondence:
Zheng Fu
e-mail: zheng.fu@lsce.ipsl.fr

Electronic supplementary material is available online at https://doi.org/10.6084/m9.figshare.c.5077595.

THE ROYAL SOCIETY PUBLISHING

Sensitivity of gross primary productivity to climatic drivers during the summer drought of 2018 in Europe

Zheng Fu[1], Philippe Ciais[1], Ana Bastos[2], Paul C. Stoy[3,4], Hui Yang[1], Julia K. Green[1], Bingxue Wang[5], Kailiang Yu[1], Yuanyuan Huang[1,23], Alexander Knohl[6], Ladislav Šigut[7], Mana Gharun[8], Matthias Cuntz[9], Nicola Arriga[10], Marilyn Roland[11], Matthias Peichl[12], Mirco Migliavacca[13], Edoardo Cremonese[14], Andrej Varlagin[15], Christian Brümmer[16], Louis Gourlez de la Motte[17], Silvano Fares[18], Nina Buchmann[8], Tarek S. El-Madany[13], Andrea Pitacco[19], Nadia Vendrame[19], Zhaolei Li[20], Caroline Vincke[21], Enzo Magliulo[22] and Franziska Koebsch[24]

[1]Laboratoire des Sciences du Climat et de l'Environnement, LSCE/IPSL, CEA-CNRS-UVSQ, Université Paris-Saclay, Gif-sur-Yvette 91191, France
[2]Department of Geography, Ludwig Maximilians University, Luisenstrasse 37, 80333 Munich, Germany
[3]Department of Biological Systems Engineering, University of Wisconsin, Madison, WI, USA
[4]Department of Land Resources and Environmental Sciences, Montana State University, Bozeman, MT, USA
[5]Key Laboratory of Ecosystem Network Observation and Modeling, Institute of Geographic Sciences and Natural Resources Research, Chinese Academy of Sciences, Beijing 100101, People's Republic of China
[6]Bioclimatology, University of Goettingen, Büsgenweg 2, 37077 Göttingen, Germany
[7]Global Change Research Institute of the Czech Academy of Sciences, Bělidla 986/4a, 60300 Brno, Czech Republic
[8]Department of Environmental Systems Science, ETH Zurich, Universitaetstrasse 2, 8092 Zurich, Switzerland
[9]AgroParisTech, Université de Lorraine, INRAE, UMR Silva, 54000 Nancy, France
[10]European Commission, Joint Research Centre (JRC), Via E. Fermi, 2479, 21027 Ispra, Italy
[11]Plants and Ecosystems, University of Antwerp, Universiteitsplein 1, 2610 Wilrijk, Belgium
[12]Department of Forest Ecology and Management, Swedish University of Agricultural Sciences, Skogsmarksgränd, 90183 Umeå, Sweden
[13]Department Biogeochemical Integration, Max Planck Institute for Biogeochemistry, Hans-Knöll-Strasse 10, 07745 Jena, Germany
[14]Environmental Protection Agency of Aosta Valley, Italy
[15]A.N. Severtsov Institute of Ecology and Evolution, Russian Academy of Sciences, Leninsky Prospect 33, 119071 Moscow, Russia
[16]Thünen-Institut für Agrarklimaschutz, Bundesallee 68, 38116 Braunschweig, Germany
[17]Gembloux Agro-Bio Tech (GxABT), Terra Teaching and Research Center, University of Liege, Gembloux, Belgium
[18]National Research Council, Institute for Bioeconomy, Rome, Italy
[19]DAFNAE, University of Padova, Viale dell'Università 16, 35020 Legnaro, Italy
[20]National Engineering Laboratory for Efficient Utilization of Soil and Fertilizer Resources, Key Laboratory of Agricultural Environment in Universities of Shandong, College of Resources and Environment, Shandong Agricultural University, Taian 271018, China
[21]Earth and Life Institute - Environmental Sciences, Université catholique de Louvain
[22]CNR – ISAFOM, via Patacca 85, 80040 Ercolano (Napoli), Italy
[23]CSIRO Oceans and Atmosphere, Aspendale 3195, Australia
[24]Universität Rostock, Landschaftsökologie und Standortkunde, 18059 Rostock, Germany

ZF, 0000-0001-7627-8824; PC, 0000-0001-8560-4943; AB, 0000-0002-7368-7806; LŠ, 0000-0003-1951-4100; MG, 0000-0003-0337-7367; MC, 0000-0002-5966-1829; EC, 0000-0002-6708-8532; CB, 0000-0001-6621-5010; TSE-M, 0000-0002-0726-7141; AP, 0000-0002-7260-6242

In summer 2018, Europe experienced a record drought, but it remains unknown how the drought affected ecosystem carbon dynamics. Using observations from 34 eddy covariance sites in different biomes across Europe, we studied the sensitivity of gross primary productivity (GPP) to environmental drivers during the summer drought of 2018 versus the reference summer of 2016. We found a greater drought-induced decline of summer GPP in grasslands (−38%) than in forests (−10%), which coincided with reduced

evapotranspiration and soil water content (SWC). As compared to the 'normal year' of 2016, GPP in different ecosystems exhibited more negative sensitivity to summer air temperature (Ta) but stronger positive sensitivity to SWC during summer drought in 2018, that is, a stronger reduction of GPP with soil moisture deficit. We found larger negative effects of Ta and vapour pressure deficit (VPD) but a lower positive effect of photosynthetic photon flux density on GPP in 2018 compared to 2016, which contributed to reduced summer GPP in 2018. Our results demonstrate that high temperature-induced increases in VPD and decreases in SWC aggravated drought impacts on GPP.

This article is part of the theme issue 'Impacts of the 2018 severe drought and heatwave in Europe: from site to continental scale'.

1. Introduction

The summer of 2018 was among the most severe summer droughts recorded in Europe in the past two decades following the 2003, 2010 and 2015 droughts [1,2] and primarily affected Central and Northern Europe which usually receive adequate moisture during summer [3]. It is imperative to understand and quantify how ecosystems respond to heat and drought stress, given the increasing likelihood of such events [4] and their detrimental impacts on ecosystems and human livelihoods [5,6].

Summer drought and heatwave affect photosynthesis primarily due to the physiological response to water deficit and high temperature, including reductions in enzymatic activity, mesophyll and stomatal conductance to prevent water loss [7,8]. These effects have been often related to air temperature (Ta), vapour pressure deficit (VPD) and soil water content (SWC) [8]. Gross primary productivity (GPP) initially increases with rising Ta but decreases above a certain optimum temperature [9] when maximum rates of carboxylation and electron transport [10] become affected. Increases in VPD will increasingly constrain stomatal conductance and thereby GPP, while SWC deficit leads to reductions in enzymatic activity or mesophyll and stomatal conductance, and thus GPP [11,12]. In addition, photosynthetic photon flux density (PPFD) is also a major factor in driving GPP during the summer; however, under drought conditions, it may be not as strong as it has been in a normal or wet year [13] because vegetation becomes water limited rather than energy limited for evapotranspiration (ET) and thus GPP. GPP is strongly impacted by these multiple climate drivers, but it remains unclear how drought impacts the sensitivity of GPP to these climate drivers, given high covariance of the above-mentioned drought drivers.

Drought and heatwave effects on GPP are complex because of multiple causal relationships among different climate variables. For example, increased Ta could directly stimulate enzyme activity and accelerate photosynthesis rate, or reduce it through the reduction of enzyme activation and capacity if temperature becomes too high [14]. But increased Ta could also indirectly affect GPP through increasing VPD (Ta → VPD → GPP), decreasing SWC via increasing ET (Ta → ET → SWC → GPP), or by involving both terms (e.g. Ta → ET → VPD → SWC → GPP) [8,15]. Increases in SWC under water-limited conditions could have a positive direct effect on GPP, but also a positive indirect effect on GPP through decreasing VPD due to atmospheric feedbacks (SWC → VPD → GPP) [12,16]. However, it remains elusive how drought and heatwave impact these causal relationships among different climate variables and what their relative influences are on GPP. Exploring the relationships between these variables will help us to elucidate some of the causality issues involved in environmental controls over GPP across different ecosystems.

With the advantage of quasi-continuous measurements of carbon and water vapour fluxes, there has been a large increase in the prevalence of eddy covariance (EC) flux towers in Europe during the last decade (http://www.europe-fluxdata.eu), progressively merging into the standardized research infrastructure ICOS (Integrated Carbon Observation System). With its representative sampling of the terrestrial biosphere's climate and ecological spaces, this regional network provides background information and direct measurements on how ecosystem metabolism responds to environmental and biological forcing [17,18], giving us a unique opportunity to study the impacts of the 2018 summer drought on ecosystem carbon cycling. In this study, we focused on the effects of the recent summer drought in 2018 and addressed the following questions: (1) How much did the GPP change during the 2018 summer drought? (2) Did the drought impact the sensitivity of GPP to climate drivers? And (3), what are the direct and indirect influences of Ta, VPD, SWC and PPFD and their interactions on GPP before and during drought?

2. Material and methods

(a) Datasets

This analysis used carbon fluxes from EC observations and meteorological data gathered through the European Flux Database and processed in the framework of the ICOS 2018 Drought initiative from the ICOS dataset [19]. Half-hourly EC data were processed, quality controlled, u*-filtered and gap-filled following standardized protocols [20]. At each site, net ecosystem exchange (NEE) was measured and partitioned into GPP and ecosystem respiration (TER) following the night-time and daytime partitioning methods [21,22]. Based on measured high-quality NEE data, GPP from the daytime partitioning method were used for sensitivity calculation and path analysis. Sites that met the following criteria were included in our analyses: (i) no disturbance within 10 years before the onset of EC measurements and non-cropland ecosystems; (ii) sites with observations during the typical summer of 2016 and the 2018 summer drought. Croplands were excluded because rotations occur at different sites, with different cultivars often planted between 2016 and 2018. This led to a final list of 34 sites across 7 vegetation types, including 15 evergreen needleleaf forests, 5 deciduous broadleaf forests, 4 mixed forests, 5 grasslands, 3 savannahs, 1 shrubland and 1 wetland (table 1 and figure 1). The choice of 2016 as a reference period is justified by the availability of high-quality data from numerous sites, and because 2016 was a normal year with precipitation near the average across most of Europe. The average summer precipitation in Europe during 1979–2018 was 697 mm while it was 688 mm in 2018. Meanwhile, some areas of continental Europe experienced drought in 2015 (especially in eastern Europe) and/or 2017 (especially in southern Europe) [23–25].

(b) Definitions and classifications

To quantify the climate and carbon flux changes in the summer drought of 2018 versus that of 2016, both the absolute (ΔX) and relative changes (δX) in each variable (X) were computed from

the data:

$$\Delta X = X_{2018} - X_{2016} \tag{2.1}$$

and

$$\delta X = \frac{X_{2018} - X_{2016}}{X_{2016}} \times 100\%, \tag{2.2}$$

where X_{2018} and X_{2016} represent the variable X during summer (June–July–August) in 2018 and 2016 for each site, respectively.

We used the summer soil water content (SWC) changes as a relative drought index for each site. In the grassland and wetland sites, a shallow root zone was considered and SWC measurements from the top 5 cm were used in the analysis, while in the shrublands and savannahs soil water measurements of up to 80–100 cm (available depth for these sites) were used. For the forests, SWC was measured at several depths at five forest sites (electronic supplementary material, figure S1), while most other forest sites only include the shallow soil water measurements (0–5 or 10 cm). We calculated a depth-weighted average soil water content using soil water content at each layer and depth of the layer in shrublands, savannahs and forests:

$$\mathrm{SWC} = \frac{2\mathrm{SWC}_1 L_1 + (\mathrm{SWC}_1 + \mathrm{SWC}_2)L_2 + (\mathrm{SWC}_2 + \mathrm{SWC}_3)L_3 + (\mathrm{SWC}_3 + \mathrm{SWC}_4)L_4 + (\mathrm{SWC}_4 + \mathrm{SWC}_5)L_5}{2 \times \sum_{i=1}^{5} L_i}, \tag{2.3}$$

where SWC refers to the profile weighted mean soil water content (%); SWC_i refers to soil water content at the ith layer (%) and L_i (i = 1, 2, …, 5) refers to the depth of the ith soil layer (cm). The sum of L_i (i = 1, 2, … , 5) is 80 cm. We fitted the model to deeper SWC (0–80 cm) and surface SWC (0–5 cm) across these five forest sites during the summer of 2018 and 2016 using an exponential function [26] (electronic supplementary material, figure S1). SWC at the forest sites missing deep SWC measurements were estimated using the surface SWC measurement and fitted model (electronic supplementary material, figure S1).

According to their relative changes of SWC, all sites were classified into three groups (table 1 and figure 1). Group 1 consisted of the 23 (68%) sites that experienced 2018 summer drought conditions with SWC at least 10% less than 2016 ($\delta\mathrm{SWC} \leq -10\%$), while there were 7 sites in Group 2 where little change in SWC occurred ($-10\% < \delta\mathrm{SWC} < 10\%$). Group 3 was defined as wet and included sites that experienced an SWC increase of at least 10% ($\delta\mathrm{SWC} \geq 10\%$, 4 sites) (table 1).

(c) Data analyses

We used the 2018 drought as a natural experiment, where 2016 was considered as the control, while 2018 was the treatment. We assumed that the sensitivities of GPP to environmental factors are different under dry and normal condition. Daily time series of GPP and environmental variables (Ta, VPD, SWC and PPFD) during summer (June–July–August) for each site were first normalized to calculate the standardized sensitivities of GPP to Ta, VPD, SWC and PPFD in 2018 and 2016. For each variable, the mean value across the summer of 2018 and 2016 was subtracted for each day at each site and then normalized by its standard deviation. After normalization, we used a linear mixed model with sites as the random factor to calculate the sensitivity of GPP to Ta, VPD, SWC and PPFD during the summer in 2018 and 2016, respectively, for each group in table 1:

$$\mathrm{GPP} = \beta_1\, Ta + \beta_2\, \mathrm{VPD} + \beta_3\, \mathrm{SWC} + \beta_4\, \mathrm{PPFD} + b + \varepsilon, \tag{2.4}$$

where β is the standardized sensitivity to each independent variable; b represents the random effect of the site; and ε is random error. The variance inflation factor (VIF) was used to quantify the degree of multicollinearity for the model [27] and a VIF < 6 for each variable was found, indicating that the degree of multicollinearity for the model was not strong. The surface conductance (G_s) in the summer of 2018 and 2016 was calculated using half-hourly data (11.00–14.00 averages, removing rainy hours) by inverting the Penman–Monteith equation [28] as shown in equation (2.5) for each site and then averaged for each group in table 1.

$$G_s = \frac{r_a \gamma}{(\Delta(R_n - G) + \rho c_p r_a (e_s(T_a) - e_a))/\lambda E - (\Delta + \lambda)}, \tag{2.5}$$

where G_s and r_a are canopy stomatal conductance and aerodynamic resistance, γ is the psychometric constant, Δ is the slope of the water vapour deficit, Rn and G are net radiation and soil heat flux, ρ is air density, C_p is specific heat capacity of dry air, e_s and e_a are saturated and actual vapour pressure, respectively, and λE is evapotranspiration. r_a is calculated following Novick *et al.* [12] (equation (2.6)), using the von Karman constant ($k = 0.4$), available wind speed data (w_s), measurement height (z_m), as well as the momentum roughness length ($z_0 =$ 0.1 h) and zero plane displacement ($z_d = 0.67$ h) both based on calculated canopy height (h) from near neutral conditions [29] (equation (2.7)).

$$r_a = \frac{\ln((z_m - z_d)/z_0)^2}{w_s k^2} \tag{2.6}$$

and

$$h = \frac{z_m}{0.6 + 0.1 \times \exp(k w_s / u^*)}. \tag{2.7}$$

Path analysis was used to evaluate the causal relationships and relative influences among different variables [30,31] and to determine the direct and indirect factors influencing GPP. By stepwise removal of non-significant paths in the initial model, we selected a final model that best fits the observations. The adequacy of the model was determined by χ^2-test and root mean squared error of approximation (RMSEA) index. The χ^2-test was used to assess whether the model reasonably explained the patterns of the data. Favourable model fits were selected by non-significant difference in the χ^2-test ($p > 0.05$) and low RMSEA (less than 0.08) following Liu *et al.* [32]. The path analysis was performed using the R package 'lavaan' [31]. Other calculations and analyses were conducted using MATLAB R2016b (The Mathworks Inc., Natick, MA, USA). A statistical probability of $p < 0.05$ was used to determine significance for all tests.

3. Results

(a) Changes in climate and ecosystem carbon fluxes between 2016 and 2018

Most sites experienced summer drought conditions in 2018 (Group 1, $\delta\mathrm{SWC} \leq -10\%$, 68% of sites). In comparison with year 2016, the mean daily summer PPFD, Ta and VPD were higher by 39 ± 5 µmol $\mathrm{m}^{-2}\,\mathrm{s}^{-1}$ (± standard error; a relative change of 10%), 1.5 ± 0.1°C (9%) and 2.4 ± 0.2 hPa (45%) at these sites, respectively, while total precipitation and SWC decreased by 111 ± 25 mm (36%) and $9.1 \pm 1.0\%$ (a relative change of 31%), respectively (table 1 and figure 1*d*). Summer

Table 1. Changes in summer climate and ecosystem CO_2 fluxes between 2018 and 2016 at the EC sites. Abbreviations: ENF, evergreen needle-leaved forests; DBF, broadleaved deciduous forests; MF, mixed forests; GRA, grasslands; SAV, savannahs; OSH, open shrubland; WET, wetland; MAT, mean annual temperature; MAP, mean annual precipitation; Ta, air temperature; VPD, vapour pressure deficit; SWC, soil water content; PPFD, photosynthetic photon flux density; P, total summer precipitation; ET, summer evapotranspiration; GPP, summer gross primary productivity; NEE, summer net ecosystem exchange; TER, summer ecosystem respiration.

				MAT	MAP	ΔTa	ΔVPD	ΔSWC	ΔPPFD	ΔP	ΔET	ΔNEE		
site ID	IGBP class.	latitude	longitude	(°C)	(mm)	(°C)	(hPa)	(%)	(μmol m^{-2} s^{-1})	(mm)	(mm)	ΔGPP	(g Cmm^{-2})	ΔTER
Group 1: δSWC ≤ −10%														
BE-Bra	MF	51.31	4.52	9.8	750	1.6	3.0	−8.4	68	−157	−13	−220	−55	−275
BE-Vie	MF	50.30	6.00	7.8	1062	1.9	3.3	−5.3	71	−109	−1	−8	−51	−59
CH-Cha	GRA	47.21	8.41	9.5	1136	1.3	3.2	−18.6	59	−311	−52	−465	−43	−508
CH-Dav	ENF	46.82	9.86	3.5	1046	1.5	1.4	−8.7	41	−470	−14	15	−140	−125
CH-Fru	GRA	47.12	8.54	7.2	1651	1.3	1.6	−13.7	49	−290	20	−81	120	39
CZ-BK1	ENF	49.50	18.54	6.7	1316	1.0	0.6	−11.3	9	41	19	147	5	152
CZ-Lnz	MF	48.68	16.95	9.3	550	1.7	3.5	−8.2	−3	−80	12	−99	−36	−135
CZ-RAJ	ENF	49.44	16.70	7.1	681	1.8	2.8	−5.5	12	−27	−70	−303	160	−143
CZ-Stn	DBF	49.04	17.97	8.7	685	1.4	1.6	−6.5	18	−137	4	32	−19	13
DE-Gri	GRA	50.95	13.51	7.8	901	1.2	3.0	−22.2	22	−73	−89	−591	66	−525
DE-Hai	DBF	51.08	10.45	8.3	720	1.8	3.8	−7.1	44	−101	−64	−416	204	−212
DE-HoH	DBF	52.09	11.22	9.1	563	1.6	2.8	−8.1	5	−56	−38	−88	−25	−113
DE-Obe	ENF	50.79	13.72	5.5	996	1.6	3.4	−15.7	25	−150	−70	−416	22	−394
FI-Hyy	ENF	61.85	24.29	3.8	709	2.0	3.5	−9.1	94	−163	8	5	−65	−60
FR-Bil	ENF	44.49	−0.96	12.8	930	1.2	−0.2	−2.8	26	5	26	−45	81	36
FR-Hes	DBF	48.67	7.06	9.2	820	1.7	3.4	−6.4	60	−158	40	32	63	95
IT-Lsn	OSH	45.74	12.75	13.1	1083	1.3	1.3	−10.8	10	20	−21	43	34	77
NL-Loo	ENF	52.17	5.74	9.8	786	1.6	1.9	−6.0	70	−183	−72	−97	39	−58
SE-Deg	WET	64.18	19.56	1.2	523	1.2	1.7	−9.0	50	−23	65	−8	27	19
SE-Htm	ENF	56.10	13.42	7.4	707	2.1	3.3	−10.4	63	−94	−24	−180	93	−87
SE-Nor	ENF	60.09	17.48	5.5	527	2.0	2.4	−6.9	23	27	4	−31	−57	−88
SE-Ros	ENF	64.17	19.74	1.8	614	0.8	2.3	−5.9	47	−1	−1	−55	58	3
SE-Svb	ENF	64.26	19.77	1.8	614	1.7	2.2	−2.8	41	−68	−18	−45	−19	−64
Group 2: −10% < δSWC < 10%														
CH-Lae	MF	47.48	8.37	8.7	1211	1.6	2.5	−1.3	37	−77	−139	−296	348	52
DE-Tha	ENF	50.96	13.57	8.2	843	1.6	3.5	−1.2	30	−87	−55	−258	107	−151
DK-Sor	DBF	55.49	11.64	8.2	660	1.8	3.1	−1.9	58	−171	−24	−375	0	−375

(*Continued*.)

Table 1. (*Continued.*)

site ID	IGBP class.	latitude	longitude	MAT (°C)	MAP (mm)	ΔTa (°C)	ΔVPD (hPa)	ΔSWC (%)	ΔPPFD (μmol m^{-2} s^{-1})	ΔP (mm)	ΔET (mm)	ΔGPP	ΔNEE (g Cmm^{-2})	ΔTER
ES-Abr	SAV	38.70	−6.79	16.3	450	−2.0	−5.4	0	−45	6	−12	−2	−12	−14
ES-LM1	SAV	39.94	−5.78	16	700	−1.0	−2.0	−1.2	−25	3	−43	15	−44	−29
ES-LM2	SAV	39.93	−5.78	16	700	−0.9	−2.2	1	−26	−4	−34	55	−27	28
IT-Tor	GRA	45.84	7.58	2.9	920	0.7	−0.4	0	10	34	−2	−6	53	47
Group 3: δSWC ≥ 10%														
CH-Aws	GRA	46.58	9.79	2.3	918	1.2	0.6	3.0	17	−203	−28	180	−76	104
IT-SR2	ENF	43.73	10.29	14.2	920	1.1	1.6	1.1	−11	−3	50	−44	68	24
RU-Fyo	ENF	56.46	32.92	3.9	711	−1.1	−1.3	22.9	−16	−66	−69	173	−13	160
RU-Fy2	ENF	56.45	32.90	3.9	711	−0.5	−0.3	21.4	−19	−35	54	310	−184	126

GPP and ecosystem respiration (TER) in 2018 decreased at most sites in Group 1 and increased in ecosystems that were wetter in 2018 in Group 3 (table 1). The decrease in GPP from Group 1 sites (-125 ± 40 g C m^{-2} season^{-1}, −14%) coincides with reduced ET (-15 ± 8 mm season^{-1}, −7%) and SWC deficits (table 1 and figure 1*d*). However, for the wetter sites in Group 3 (δSWC ≥ 10%), the relative change of SWC and Ta increased by 33% and 2% on average, respectively, leading to increases of GPP and ET by 19% and 5%, respectively.

The drought in 2018 had a stronger impact on summer GPP, TER and ET of grasslands compared to forest sites. For the grassland sites in Group 1 (δSWC ≤ −10%), GPP and TER decreased by 379 ± 153 (38%) and 331 ± 185 (33%) g C m^{-2} season^{-1}, respectively (table 1). Mean GPP and TER in forests decreased by 98 ± 32 (10%) and 84 ± 27 (14%) g C m^{-2} season^{-1}, respectively. Also, summer ET decreased by 41 ± 32 (15%) mm season^{-1} in grasslands compared to a reduction by 15 ± 7.2 (9%) mm season^{-1} in forests for Group 1 (table 1 and figure 1*d*). The reduction of mean summer TER (-105 ± 37 g C m^{-2} season^{-1}) is on average lower than that of GPP (-125 ± 40 g C m^{-2} season^{-1}), causing a reduction of net carbon uptake in Group 1 (table 1).

(b) Sensitivity of GPP to climate drivers in 2018 and 2016

The summer drought in 2018 impacted the sensitivity of GPP to climate drivers as compared to 2016 (figure 2). In Group 1, the sensitivity of GPP to Ta was significantly positive in the summer of 2016 (0.15 ± 0.03) but it was close to zero in 2018 (-0.03 ± 0.03, figure 2*a*). GPP was four times more sensitive to SWC in the summer of 2018 (0.24 ± 0.03) compared to 2016 (0.06 ± 0.03, figure 2*a*). The sensitivities to VPD in 2018 and 2016 were close to −0.30 and constrained the GPP consistently during both summers. On the other hand, the mean surface conductance in 2018 (0.53 ± 0.06 cm s^{-1}) was significantly lower than that of 2016 (0.85 ± 0.05 cm s^{-1}), suggesting a stronger stomatal closure in 2018 in response to elevated VPD. Meanwhile, the positive sensitivity of GPP to PPFD in 2018 (0.62 ± 0.02) was smaller than that of 2016 (0.68 ± 0.03) in Group 1 (figure 2*a*).

GPP was negatively related to Ta in Group 2 in 2018 (-0.16 ± 0.07, figure 2*b*) due in part to the three savanna sites in this group (against no savannas in Group 1; table 1 and figure 1*b*). Although the SWC deficits were less than 10% in those savannah sites (δSWC = −6%, figure 1*d*), their summer maximum Ta were higher than 34°C, so that Ta had a strong negative effect on GPP. When we removed the savannah sites in Group 2, there was no significant difference between 2018 and 2016 for the sensitivity of GPP to climate in this group (electronic supplementary material, figure S2). In contrast to Group 1, Group 3 was less sensitive to SWC in 2018 (0.14 ± 0.05) than in 2016 (0.51 ± 0.06) because of higher SWC in 2018 at these sites (figure 2*c*). The sensitivity of GPP to Ta in the summer of 2018 (0.16 ± 0.05) was significantly positive in Group 3 (figure 2*c*).

We further classified Group 1 into different vegetation types and found weaker and even negative Ta sensitivities in 2018 compared to 2016 across all vegetation types, including evergreen needleleaf forests, deciduous broadleaf forests, mixed forests, grasslands, shrubland and wetland (figure 3). Results also showed that the positive sensitivity of GPP to SWC in 2018 was stronger than that of 2016 in all vegetation types

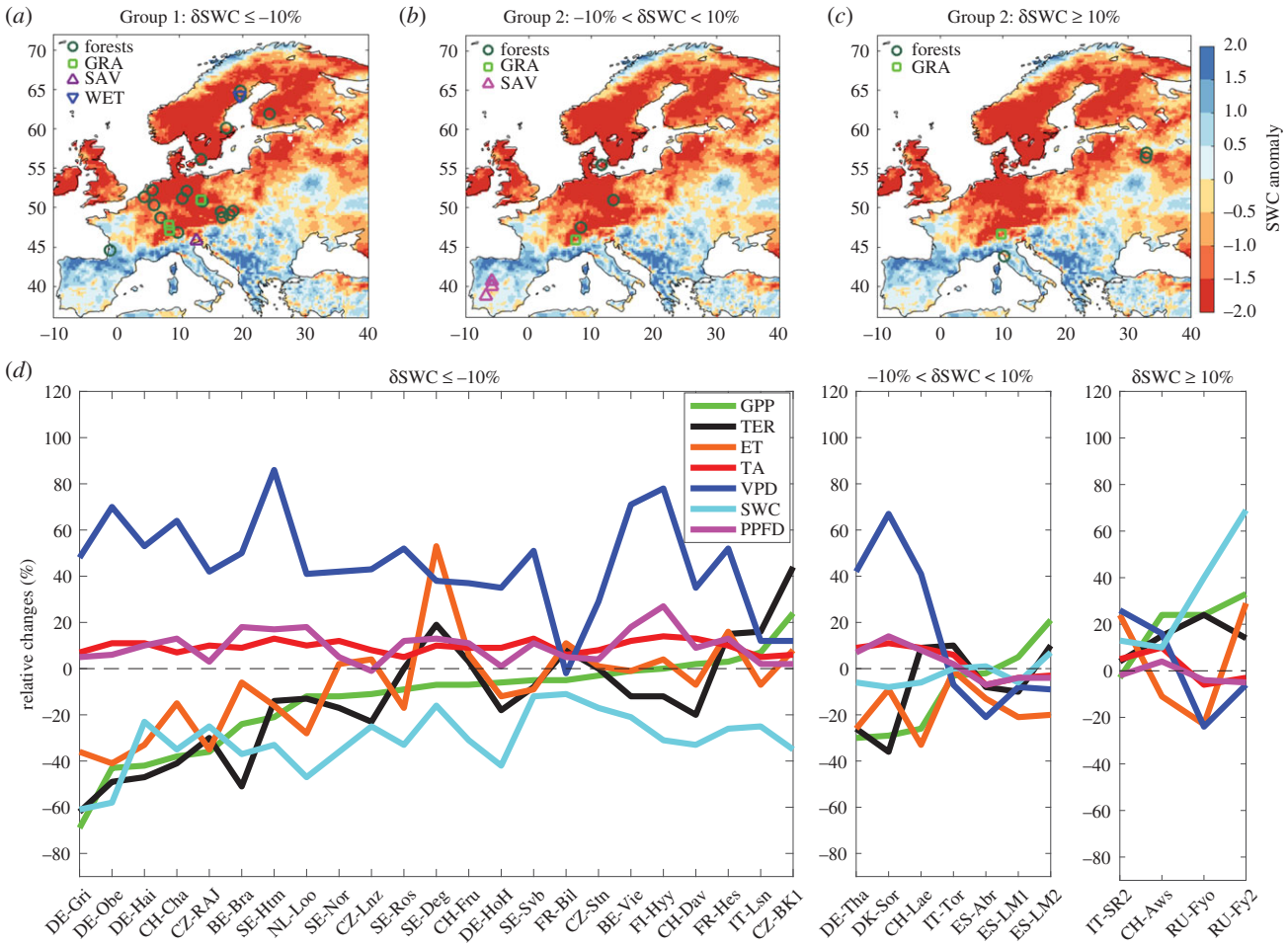

Figure 1. Distribution map of EC sites in Group 1 (*a*), Group 2 (*b*), Group 3 (*c*) and the relative changes (*d*) of climate and ecosystem carbon fluxes in the summer of 2018 when referred to the typical summer of 2016 at the three groups of EC sites. Ecosystems are sorted by relative change in GPP from the most negative to the most positive values. The background map is the spatial distribution of summer soil water content (SWC, 0–289 cm) anomaly in 2018 (*z*-score) when referred to 1979–2018, and it was calculated using the atmospheric reanalysis from the European Center for Medium-range Weather Forecast (ECMWF), the ERA5 Reanalysis, which provides climate fields at 0.25° spatial and hourly temporal resolution from 1979 until the present. GPP, gross primary productivity; TER, ecosystem respiration; ET, summer evapotranspiration; Ta, air temperature; VPD, vapour pressure deficit; PPFD, summer photosynthetic photon flux density. (Online version in colour.)

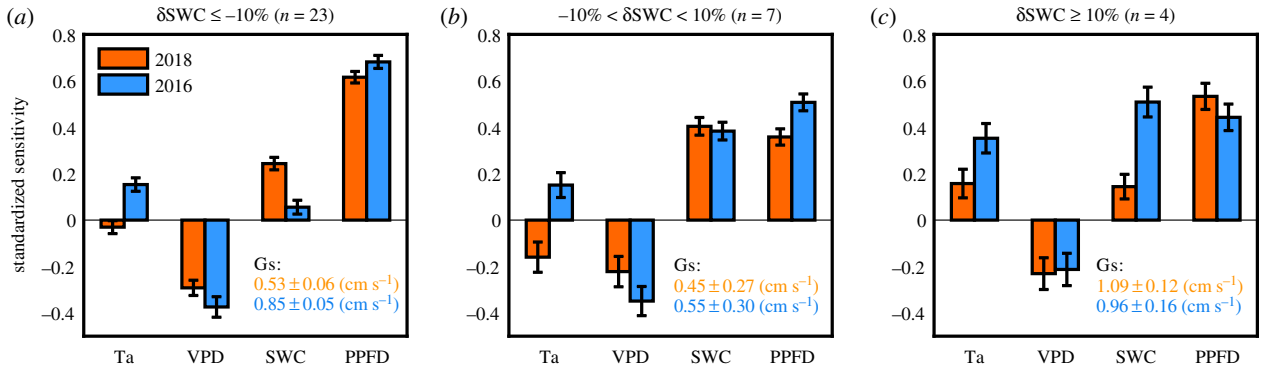

Figure 2. Standardized sensitivity of GPP to air temperature (Ta), vapour pressure deficit (VPD), soil water content (SWC) and photosynthetic photon flux density (PPFD) during the summers of 2018 and 2016 under different SWC changes. Error bars represent ±1 standard error. Insert numbers are mean surface conductance (G_s, ± standard error) in the summer of 2018 (orange) and 2016 (blue). (Online version in colour.)

except for the wetland; GPP was not sensitive to SWC in wetland in both 2018 and 2016 (figure 3). Meanwhile, we found the change patterns in sensitivities of ET to climate drivers were similar to that of GPP for different vegetation types in Group 1 (electronic supplementary material, figure S3). ET had weaker sensitivity to Ta and PPFD but stronger sensitivity to SWC in 2018 than that of 2016 in forests, grasslands and shrubland (electronic supplementary material, figure S3).

(c) Relative influences of climate drivers on gross primary productivity

The path analysis showed that the direct, indirect and total effects of each climate factor on GPP during the summer were different between 2018 (figure 4*a*,*c*) and 2016 (figure 4*b*,*d*) across all of the sites in Group 1 (δSWC ≤ −10%) except for wetland. The direct effect of Ta on GPP was

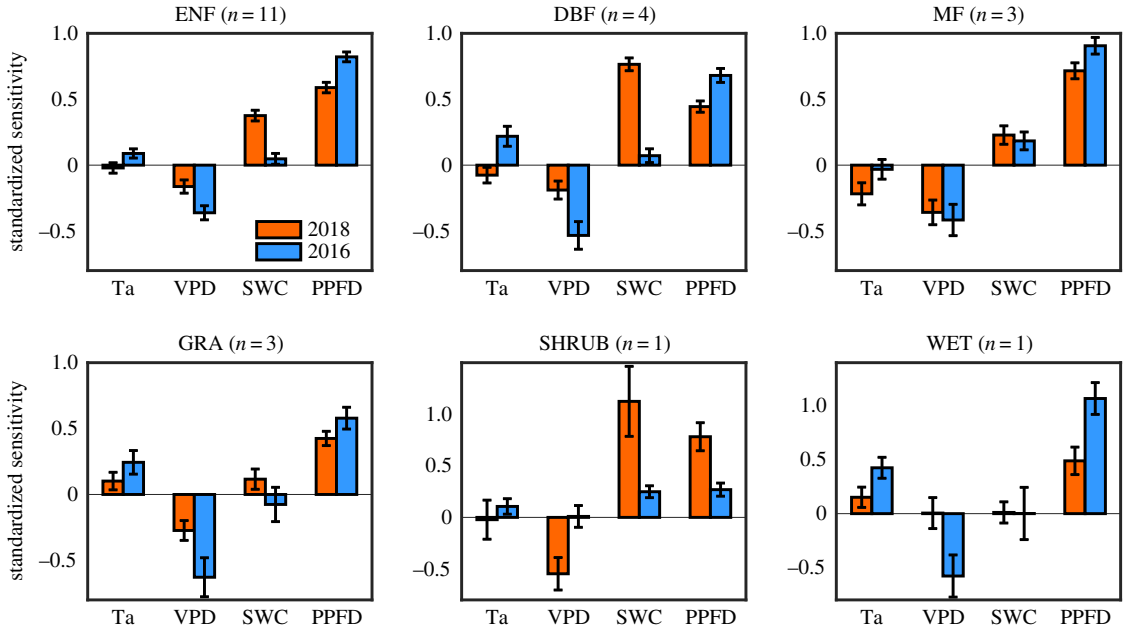

Figure 3. Standardized sensitivity of GPP to Ta, VPD, SWC and PPFD during the summers of 2018 and 2016 for different vegetation types in Group 1 (δSWC ≤ −10%). Error bars represent ±1 standard error. ENF, evergreen needle-leaved forests; DBF, broadleaved deciduous forests; MF, mixed forests; GRA, grasslands; SHRUB, shrubland; WET, wetland. (Online version in colour.)

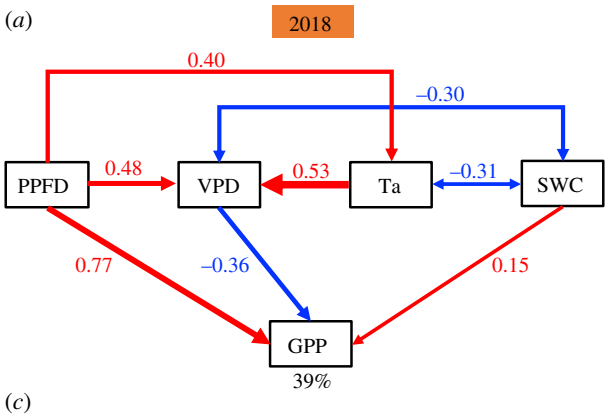

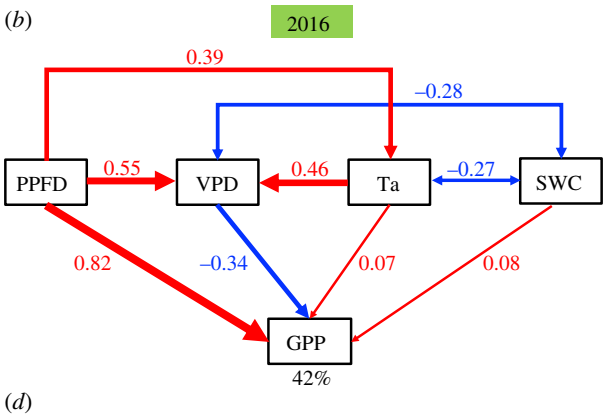

(c)

climate	direct effect in 2018	causal relationships	indirect effect in 2018	total effect in 2018
Ta	ns	Ta → VPD → GPP	−0.19	−0.29
		Ta → SWC → GPP	−0.05	
		Ta → SWC → VPD → PP	−0.03	
		Ta → VPD → SWC → GPP	−0.02	
VPD	−0.36	VPD → SWC → GPP	−0.05	−0.41
		VPD → SWC → Ta → GPP	n.s.	
SWC	0.15	SWC → VPD → GPP	0.11	0.32
		SWC → Ta → GPP	n.s.	
		SWC → Ta → VPD → GPP	0.06	
PPFD	0.77	PPFD → VPD → GPP	−0.17	0.48
		PPFD → Ta → VPD → GPP	−0.08	
		PPFD → Ta → VPD → SWC → GPP	−0.01	
		PPFD → Ta → SWC → VPD → GPP	−0.01	
		PPFD → Ta → GPP	n.s.	
		PPFD → Ta → SWC → GPP	−0.02	

(d)

climate	direct effect in 2016	causal relationships	indirect effect in 2016	total effect in 2016
Ta	0.07	Ta → VPD → GPP	−0.16	−0.15
		Ta → SWC → GPP	−0.02	
		Ta → SWC → VPD → GPP	−0.03	
		Ta → VPD → SWC → GPP	−0.01	
VPD	−0.34	VPD → SWC → GPP	−0.02	−0.36
		VPD → SWC → Ta → GPP	0.005	
SWC	0.08	SWC → VPD → GPP	0.10	0.20
		SWC → Ta → GPP	−0.02	
		SWC → Ta → VPD → GPP	0.04	
PPFD	0.82	PPFD → VPD → GPP	−0.19	0.58
		PPFD → Ta → VPD → GPP	−0.06	
		PPFD → Ta → VPD → SWC → GPP	−0.004	
		PPFD → Ta → SWC → VPD → GPP	−0.01	
		PPFD → Ta → GPP	0.03	
		PPFD → Ta → SWC → GPP	−0.008	

Figure 4. Path analysis effect of climatic variables on GPP during the summer of 2018 (*a*) and 2016 (*b*) across all of sites under δSWC ≤ −10% (i.e. Group 1) except the wetland site. Direct, indirect and total effects of Ta, VPD, SWC and PPFD on GPP from path analysis and the paths for driving GPP in 2018 (*c*) and 2016 (*d*). Red and blue arrows represent the positive and negative effects in a fitted structural equation model, respectively. The widths of the arrows indicate the strength of the causal relationship. Percentages (R^2) underneath GPP values indicate the variance explained by climatic factors during the summer. The standardized total effect of each climate factor on GPP is equal to the sum of direct and indirect effects (n.s., not significant). (Online version in colour.)

positive (0.07 ± 0.02) in 2016 (figure 4*b*) but not significant in 2018 (figure 4*a*). The direct positive effect of SWC in 2018 (0.15 ± 0.03) was higher than in 2016 (0.08 ± 0.03) while VPD had a direct negative effect on GPP both in the summer of 2018 (−0.36, figure 4*a*) and 2016 (−0.34, figure 4*b*). PPFD had a smaller direct positive effect on GPP in 2018 (0.77 ± 0.03) than that of 2016 (0.82 ± 0.03).

As for indirect effects, Ta had an indirect negative effect on GPP through VPD and SWC during both summers in 2018 (−0.19 and −0.05, figure 4*c*) and 2016 (−0.16 and −0.02, figure 4*d*).

Ta had a strong indirect negative effect on GPP (−0.29, figure 4*c*) due to its impact on VPD and SWC in 2018 but no direct positive effect on GPP, thus resulting in a strong total negative effect (−0.29). In 2016, the direct positive effect of Ta on GPP was 0.07 and partly offset the indirect negative effect through VPD and SWC (figure 4*d*), so its total effect was only −0.15. Increased VPD in 2018 reduced SWC and had an indirect negative effect on GPP (−0.05), which further enhanced the negative direct effect of VPD on GPP, leading to a large negative total effect (−0.41). The indirect positive effects of SWC on GPP were 0.11 and 0.06 through its role in decreasing VPD and Ta, respectively, in 2018 (figure 4*c*). PPFD had an indirect negative or positive effect on GPP through increasing VPD and Ta, respectively, both in 2018 and 2016. Overall, the total effects from Ta, VPD, SWC and PPFD on GPP in 2018 (figure 4*c*) were −0.29, −0.41, 0.32 and 0.48, respectively, while they were −0.15, −0.36, 0.20 and 0.58, respectively, in 2016 (figure 4*d*). Thus, larger negative effects from Ta and VPD but lower positive effect from PPFD in the summer of 2018 than that of 2016 led to a summer GPP reduction in 2018.

4. Discussion

(a) Drought and ecosystem carbon fluxes in 2018

Our results show that most sites in Group 1 experienced a GPP reduction in the summer of 2018 despite inter-site differences in drought duration, soil characteristics, vegetation state and species-specific responses to climate variation. The exceptionally high temperature, which increased VPD, and the lack of precipitation, which reduced soil water availability, resulted in a decrease of summer GPP and ET. The response of carbon fluxes to drought stress is tightly coupled with soil water availability and stomatal regulation [33]. During drought stress, soil moisture deficit results in more negative soil water potentials, that translate into more negative root, stem and leaf water potentials. In case the evaporative demand is high and evaporative supply cannot be controlled by xylem conductance and stomatal closure, stem water potentials drop below a threshold representing a 50% loss of conductance, and cavitation and embolism can happen, leading to a long-lasting decline in GPP and mortality [34,35]. On the other hand, stomatal control optimizes marginal water loss per carbon gain and can reduce GPP in the short term [35].

We also found that TER decreased together with GPP at most sites in Group 1 (table 1 and figure 1*d*). A reduction in both plant respiration (due to diminished substrates) and microbial soil respiration (due to diminished substrates from plants and microbial response to drought) can explain such parallel TER and GPP responses [36,37]. Burton *et al.* [37] reported that drought reduced root autotrophic respiration by affecting carbon allocation. Since exudates and carbon substrate provided to soil decomposers from GPP (e.g. fine root turnover) is reduced during drought, there is also a possible contribution of GPP to the reduction of soil heterotrophic respiration. In addition, lower SWC may limit soil respiration and its response to soil temperature changes [38,39]. Vegetation models typically predict that warmer temperatures increase both microbial and plant respiration, but generally differ in their parametrization of water-limitation on microbial respiration [40,41]. To better understand the response of autotrophic and heterotrophic respiration to drought, microbial and root respiration should be measured during the drought.

Relative changes in summer GPP and TER vary among biomes due to different resistances to drought. Forest ecosystems tend to have deeper roots and are more isohydric as compared to grasslands [42,43]. Therefore, they tend to be more resistant to early stages of drought if they can tap soil water throughout their rooting zone [44]. Several sites in Group 1 showed increased GPP and TER in spite of reduced SWC (e.g. CZ-BK1) which might be caused by the legacy effects of spring abnormally high leaf area and water-use efficiency dynamics mediated by vegetation composition [45]. Meanwhile, warmer temperatures also might stimulate photosynthesis and microbial activity at cold and high-latitude sites with high mean annual precipitation (greater than 1300 mm at CZ-BK1). In addition, the net carbon uptake was enhanced at some sites in Group 1, which results from the imbalance between GPP and TER in response to drought. At sites where TER is more sensitive to drought than GPP, drought could increase the net carbon uptake. In a long-term field experiment, Jentsch *et al.* [46] imposed an extreme drought in a grassland and reported that drought decreased soil respiration without reducing net primary production. Moreover, we found that the correlation coefficient between δGPP and δSWC was higher for deeper soil moisture, whereas δTER was more correlated with surface moisture (electronic supplementary material, table S1). This result suggests that GPP responds to deeper SWC and TER responds to surface SWC as most of the litter and soil organic carbon is in the topsoil, and their different responses to SWC at different depths determines the change of net carbon uptake controlled by SWC.

It should be also noted that the results are sensitive to the choice of the reference year because we only compared the 2018 data to the 2016 observed values and not to a long-term average. Due to the different time coverage of observations with few long-term sites, and considering the choice of 2016 versus 2015 or 2017 as a reference, we found some areas of continental Europe experienced drought in 2015 and/or 2017 [23–25]. This justified our choice of 2016 as a reference year.

(b) Sensitivity of gross primary productivity to climate drivers during the summer drought

Distinctive sensitivities of GPP to Ta, SWC and PPFD were found during 2018 summer as compared with summer 2016 in Group 1 (δSWC ≤ −10%). Increasing temperature stimulates enzyme activity and accelerates photosynthesis rate during the growing season in the normal year [47]. But exceptionally high temperature could reduce GPP through the reduction of enzyme (Rubisco) activation and capacity, especially in dry conditions when leaf temperatures are elevated in the absence of transpiration cooling [14,48,49]. Our results across all vegetation types in Group 1 showed weaker—and even negative—Ta sensitivities in 2018 than those of 2016, indicating that the drought and heatwave changed the response strength of GPP to Ta. Increase in Ta also translates into an increase in VPD if atmospheric humidity remains constant, and VPD serves as a strong control over GPP [50]. This study showed that VPD stress can still take place without soil moisture limitation because GPP had a similar magnitude of negative sensitivity to VPD in 2018 as in 2016, which is supported by the recent findings. For example, Novick *et al.* [12] reported VPD limited carbon and water fluxes even in mesic forests. However, our result also shows a stronger G_s closure in 2018

in response to elevated VPD, and it may be because of being partly compensated by an increase of the difference between leaf and atmospheric partial pressure of CO_2 so that the sensitivity of GPP to VPD remained constant between the two years. Additionally, we found that GPP was four times more sensitive to SWC in the summer of 2018 compared to 2016 in Group 1, revealing a strong water limitation during the drought, and possibly nonlinear response of GPP to SWC deficits [51]. This higher sensitivity of GPP to SWC during dry periods may explain why the vegetation of semi-arid ecosystems can appreciably increase carbon uptake when a sudden precipitation event occurs [52]. Plants living in semi-arid ecosystems often opportunistically respond to rainfall events, which thereby determines productivity because of the high sensitivity of GPP to SWC under dry conditions [53]. In the normal year, PPFD is usually the most important driver in controlling the summer GPP, especially in forests [13,50], but drought lowered the positive sensitivity of GPP to PPFD in the summer of 2018, which demonstrated that drought decreased radiation use efficiency and thus constrained vegetation productivity.

Not only did drought alter the sensitivities of GPP to different climatic drivers, but there was also a similar change in sensitivities of ET to climate drivers among different vegetation types in Group 1 (electronic supplementary material, figure S3). It is well documented that GPP and ET are tightly coupled [8,9,12,16,17,54], but our results from different vegetation types consistently suggest that the changes and responses in sensitivity of GPP and ET to different climatic drivers during the summer drought are also coupled. Those coupled changes have profound implications for the predictions of the carbon and water cycles in the future. Considering the GPP and ET together would be needed to better understand the impact of high temperature, VPD and the occurrence of intense droughts on ecosystems.

(c) Relative influences of climate drivers on gross primary productivity

Different climate drivers impacted the summer GPP through different pathways and we attempted to quantify their direct and indirect influences on GPP. We found that high Ta had strong indirect negative effects on GPP in 2018 due to its impacts on VPD (−0.19, Ta → VPD → GPP), while the indirect effect from Ta through decreasing SWC was relatively small (−0.05, Ta → SWC → GPP), as shown in figure 4. The ratio between these two indirect negative effects was as high as a factor of 4. High Ta determines VPD more directly than SWC because Ta positively forces ET and then affects SWC. These results are supported by recent observational and modelling studies, which emphasized that VPD has a greater effect on vegetation productivity than that of SWC [12,55]. High VPD in 2018 also further decreased SWC and led to a negative indirect effect on GPP (VPD → SWC → GPP). In turn, SWC lowered VPD and Ta by ET, and then had a positive effect on GPP. In 2016, because there was sufficient soil water availability and the Ta was not high (table 1 and figure 1*d*), SWC had less impact on GPP and Ta had a positive direct effect on GPP. In 2018, the indirect negative effect of PPFD offsets about one half its direct positive effect on GPP, leading to less total positive effect than that of 2016. The evaluation of indirect/direct effects among different variables are helpful to explain the varying magnitudes and directions of the observed carbon–climate feedback.

Climate factors only explained 39% and 42% variance in GPP in the drought and normal summer, respectively, which may result from the following two reasons. First, the spatial variability among different sites across Europe cannot be explained, although the path analysis only focused on Group 1 and excluded wetland. The inter-site differences in drought intensity and duration, soil characteristics, vegetation state and species-specific responses to climate variation are difficult to explain [25]. Second, drought also affects plant photosynthesis through changes in the vegetation canopy, such as leaf withering and senescence [56]; in other words, the biotic response to climate, rather than climate alone, is also important to explain the variation of GPP [57].

The 2018 European drought offers us a unique opportunity to study drought impacts on the ecosystem carbon cycle, including in regions that seldom experience severe drought. Our study demonstrates that high temperature-induced increases in VPD and decreases in SWC aggravated drought effects on GPP. These observed different sensitivities of GPP to climatic drivers have important implications for improving the capacity of model simulation of sensitivity of ecosystem carbon dynamics to increasing warming and drying. It is largely unknown whether land surface models can capture these changes in sensitivity to climate under drought and whether they simulate correctly the limitation of GPP and TER by water. Future studies would need to compare the model performances with observations and explore approaches for improving the simulation capability of models or their constraints.

5. Summary

This study examined how carbon fluxes responded to the 2018 drought using EC observations across Europe. We investigated the sensitivities and relative influences of different climate drivers on GPP during the summer drought of 2018 versus the reference summer of 2016. The results showed that summer TER decreased in parallel with GPP at most sites during the drought and there was a greater drought-induced decline of summer GPP in grasslands than in forests, which coincided with reduced ET and SWC. Drought also changed the sensitivity of GPP to different climate drivers. Different ecosystems consistently showed that GPP had more negative sensitivity to Ta in 2018 compared to 2016, but higher positive sensitivity to SWC during 2018. We also found larger negative effects from VPD but a lower positive effect from PPFD in the summer of 2018 than that of 2016, which contributed to reduced summer GPP in 2018. These observed different influences and sensitivities enrich our understanding of temperature–moisture interactions and help to disentangle how they affect ecosystem carbon cycling and its feedback to climate change.

Data accessibility. DOI of the dataset used in this study is: 10.18160/PZDK-EF78. Link: https://meta.icos-cp.eu/collections/UZw8ra7O-Vilm VjATTCgIimpz.

Authors' contributions. Z.F., P.C. and A.B. designed the study. Z.F. carried out the analyses. A.K., L.S., M.G., M.C., N.A., M.R., M.P., M.M., E.C., A.V., C.B., S.F., N.B., T.E.M., A.P., N.V., C.V., E.M. and F.K. contributed ecosystem flux data. All authors commented on and contributed to the final manuscript.

Competing interests. We declare we have no competing interests.

Funding. P.C. acknowledges support from the European Research Council Synergy project SyG-2013–610028 IMBALANCE-P and the ANR CLAND Convergence Institute. P.C.S. acknowledges support from

the U.S. National Science Foundation award #1552976. T.S.E.M. and M.M. thank the Alexander von Humbold Stiftung for financial support of the MaNiP project. M.G. acknowledges funding by Swiss National Science Foundation project ICOS-CH Phase 2 20FI20_173691. A.V. thanks the RFBR project (19-04-01234-a). M.C. acknowledges the support by successive European projects, by European regional development programmes with the Region Lorraine, by GIP Ecofor and SOERE F-ORE-T, by ADEME, and by the INRA Department of Forest, Grassland and Freshwater Ecology. A.P. acknowledges funding from the University of Padova (grant no. CDPA148553, 2014) for the operation of IT-Lsn. N.V. was partially supported by project VitiSOM (LIFE15 ENV/IT/000392). M.R. acknowledges the financial support of the Research Foundation-Flanders to the ICOS infrastructure. L.Š. was supported by the Ministry of Education, Youth and Sports of the Czech Republic within the CzeCOS program, grant no. LM2015061, and by SustES-Adaptation strategies for sustainable ecosystem services and food security under adverse environmental conditions (grant no. CZ.02.1.01/0.0/0.0/16_019/0000797). FR-Hes acknowledges the support by successive European projects, by European regional development programs with the Region Lorraine, by GIP Ecofor and SOERE F-ORE-T, by ADEME, and by the INRA Department of Forest, Grassland and Freshwater Ecology. M.C. acknowledges support by a grant overseen by the French National Research Agency (ANR) as part of the 'Investissements d'Avenir' program (grant no. ANR-11-LABX-0002-01, LabEx ARBRE).

Acknowledgements. We would like to thank the ICOS Infrastructure and site investigators for support in collecting and curating the EC-data for 2018.

References

1. Buras A, Rammig A, Zang CS. 2019 Quantifying impacts of the drought 2018 on European ecosystems in comparison to 2003. *arXiv* 1906.08605. (doi:10.5194/bg-2019-286-supplement)
2. Sousa PM, Barriopedro D, Ramos AM, García-Herrera R, Espírito-Santo F, Trigo RM. 2019 Saharan air intrusions as a relevant mechanism for Iberian heatwaves: the record breaking events of August 2018 and June 2019. *Weather Clim. Extremes* **26**, 100224. (doi:10.1016/j.wace.2019.100224)
3. Van der Schrier G, Briffa K, Jones P, Osborn T. 2006 Summer moisture variability across Europe. *J. Clim.* **19**, 2818–2834. (doi:10.1175/JCLI3734.1)
4. Seneviratne SI, Lüthi D, Litschi M, Schär C. 2006 Land–atmosphere coupling and climate change in Europe. *Nature* **443**, 205. (doi:10.1038/nature05095)
5. Zscheischler J, Reichstein M, Harmeling S, Rammig A, Tomelleri E, Mahecha MD. 2014 Extreme events in gross primary production: a characterization across continents. *Biogeosciences* **11**, 2909–2924. (doi:10.5194/bg-11-2909-2014)
6. Humphrey V, Zscheischler J, Ciais P, Gudmundsson L, Sitch S, Seneviratne SI. 2018 Sensitivity of atmospheric CO_2 growth rate to observed changes in terrestrial water storage. *Nature* **560**, 628–631. (doi:10.1038/s41586-018-0424-4).
7. Reichstein M *et al.* 2013 Climate extremes and the carbon cycle. *Nature* **500**, 287–295. (doi:10.1038/nature12350)
8. Seneviratne SI, Corti T, Davin EL, Hirschi M, Jaeger EB, Lehner I, Orlowsky B, Teuling AJ. 2010 Investigating soil moisture–climate interactions in a changing climate: a review. *Earth Sci. Rev.* **99**, 125–161. (doi:10.1016/j.earscirev.2010.02.004)
9. Bonan GB. 2008 Forests and climate change: forcings, feedbacks, and the climate benefits of forests. *Science* **320**, 1444–1449. (doi:10.1126/science.1155121)
10. von Buttlar J *et al.* 2018 Impacts of droughts and extreme temperature events on gross primary production and ecosystem respiration: a systematic assessment across ecosystems and climate zones. *Biogeosciences* **15**, 1293–1318. (doi:10.5194/bg-15-1293-2018).
11. Konings A, Williams A, Gentine P. 2017 Sensitivity of grassland productivity to aridity controlled by stomatal and xylem regulation. *Nat. Geosci.* **10**, 284. (doi:10.1038/ngeo2903)
12. Novick KA *et al.* 2016 The increasing importance of atmospheric demand for ecosystem water and carbon fluxes. *Nat. Clim. Change* **6**, 1023. (doi:10.1038/nclimate3114)
13. Goodrich J, Campbell D, Clearwater M, Rutledge S, Schipper L. 2015 High vapor pressure deficit constrains GPP and the light response of NEE at a Southern Hemisphere bog. *Agric. For. Meteorol.* **203**, 54–63. (doi:10.1016/j.agrformet.2015.01.001)
14. Luo Y. 2007 Terrestrial carbon-cycle feedback to climate warming. *Annu. Rev. Ecol. Evol. Syst.* **38**, 683–712. (doi:10.1146/annurev.ecolsys.38.091206.095808)
15. Jung M *et al.* 2010 Recent decline in the global land evapotranspiration trend due to limited moisture supply. *Nature* **467**, 951. (doi:10.1038/nature09396)
16. Gentine P, Green JK, Guérin M, Humphrey V, Seneviratne SI, Zhang Y, Zhou S. 2019 Coupling between the terrestrial carbon and water cycles—a review. *Environ. Res. Lett.* **14**, 083003. (doi:10.1088/1748-9326/ab22d6)
17. Baldocchi DD. 2020 How eddy covariance flux measurements have contributed to our understanding of *Global Change Biology*. *Glob. Change Biol.* **26**, 242–260. (doi:10.1111/gcb.14807)
18. Mahecha MD *et al.* 2017 Detecting impacts of extreme events with ecological in situ monitoring networks. *Biogeosciences* **14**, 4255–4277. (doi:10.5194/bg-14-4255-2017)
19. Drought 2018 Team and ICOS Ecosystem Thematic Centre. 2019 *Drought-2018 ecosystem eddy covariance flux product in FLUXNET-archive format - release 2019–1*. ICOS Carbon Portal. (doi:10.18160/PZDK-EF78)
20. Sabbatini S *et al.* 2018 Eddy covariance raw data processing for CO_2 and energy fluxes calculation at ICOS ecosystem stations. *Int. Agrophys.* **32**, 495–515. (doi:10.1515/intag-2017-0043)
21. Lasslop G, Reichstein M, Papale D, Richardson AD, Arneth A, Barr A, Stoy P, Wohlfahrt G. 2010 Separation of net ecosystem exchange into assimilation and respiration using a light response curve approach: critical issues and global evaluation. *Glob. Change Biol.* **16**, 187–208. (doi:10.1111/j.1365-2486.2009.02041.x)
22. Reichstein M *et al.* 2005 On the separation of net ecosystem exchange into assimilation and ecosystem respiration: review and improved algorithm. *Glob. Change Biol.* **11**, 1424–1439. (doi:10.1111/j.1365-2486.2005.001002.x)
23. Ionita M, Tallaksen L, Kingston D, Stagge J, Laaha G, Van Lanen H, Scholz P, Chelcea S, Haslinger K. 2017 The European 2015 drought from a climatological perspective. *Hydrol. Earth Syst. Sci.* **21**, 1397–1419. (doi:10.5194/hess-21-1397-2017)
24. Laaha G *et al.* 2017 The European 2015 drought from a hydrological perspective. *Hydrol. Earth Syst. Sci.* **21**, 3001–3024. (doi:10.5194/hess-21-3001-2017)
25. Rita A *et al.* 2020 The impact of drought spells on forests depends on site conditions: the case of 2017 summer heat wave in southern Europe. *Glob. Change Biol.* **26**, 851–863. (doi:10.1111/gcb.14825)
26. Albergel C *et al.* 2008 From near-surface to root-zone soil moisture using an exponential filter: an assessment of the method based on in-situ observations and model simulations. *Hydrol. Earth Syst. Sci.* **12**, 1323–1337. (doi:10.5194/hess-12-1323-2008)
27. Schroeder MA, Lander J, Levine-Silverman S. 1990 Diagnosing and dealing with multicollinearity. *West. J. Nurs. Res.* **12**, 175–187. (doi:10.1177/019394599001200204)
28. Monteith J. 1981 Evaporation and surface temperature. *Q. J. R. Meteorol. Soc.* **107**, 1–27. (doi:10.1002/qj.49710745102)
29. Pennypacker S, Baldocchi D. 2016 Seeing the fields and forests: application of surface-layer theory and flux-tower data to calculating vegetation canopy height. *Boundary Layer Meteorol.* **158**, 165–182. (doi:10.1007/s10546-015-0090-0)
30. Li CC. 1975 *Path analysis—a primer*. Pacific Grove, CA: Boxwood Press.
31. Rosseel Y. 2012 Lavaan: an R package for structural equation modeling and more. Version 0.5–12 (BETA). *J. Stat. Softw.* **48**, 1–36. (doi:10.18637/jss.v048.i02)
32. Liu Y, He N, Zhu J, Xu L, Yu G, Niu S, Sun X, Wen X. 2017 Regional variation in the temperature sensitivity of soil organic matter decomposition in China's forests and grasslands. *Glob.*

Change Biol. **23**, 3393–3402. (doi:10.1111/gcb.13613)

33. Thomas CK, Law BE, Irvine J, Martin JG, Pettijohn JC, Davis KJ. 2009 Seasonal hydrology explains interannual and seasonal variation in carbon and water exchange in a semiarid mature ponderosa pine forest in central Oregon. *J. Geophys. Res.* **114**, G04006. (doi:10.1029/2009JG001010)
34. Blackman CJ, Brodribb TJ, Jordan GJ. 2009 Leaf hydraulics and drought stress: response, recovery and survivorship in four woody temperate plant species. *Plant Cell Environ.* **32**, 1584–1595. (doi:10.1111/j.1365-3040.2009.02023.x)
35. Brodribb TJ, Powers J, Cochard H, Choat B. 2020 Hanging by a thread? Forests and drought. *Science* **368**, 261–266. (doi:10.1126/science.aat7631)
36. Borken W, Savage K, Davidson EA, Trumbore SE. 2006 Effects of experimental drought on soil respiration and radiocarbon efflux from a temperate forest soil. *Glob. Change Biol.* **12**, 177–193. (doi:10.1111/j.1365-2486.2005.001058.x)
37. Burton AJ, Pregitzer KS, Zogg GP, Zak DR. 1998 Drought reduces root respiration in sugar maple forests. *Ecol. Appl.* **8**, 771–778. (doi:10.1890/1051-0761(1998)008[0771:DRRRIS]2.0.CO;2)
38. Jassal RS, Black TA, Novak MD, Gaumont-Guay D, Nesic Z. 2008 Effect of soil water stress on soil respiration and its temperature sensitivity in an 18-year-old temperate Douglas-fir stand. *Glob. Change Biol.* **14**, 1305–1318. (doi:10.1111/j.1365-2486.2008.01573.x)
39. Wen X-F, Yu G-R, Sun X-M, Li Q-K, Liu Y-F, Zhang L-M, Ren C-Y, Fu Y-L, Li Z-Q. 2006 Soil moisture effect on the temperature dependence of ecosystem respiration in a subtropical *Pinus* plantation of southeastern China. *Agric. For. Meteorol.* **137**, 166–175. (doi:10.1016/j.agrformet.2006.02.005)
40. Koven CD, Hugelius G, Lawrence DM, Wieder WR. 2017 Higher climatological temperature sensitivity of soil carbon in cold than warm climates. *Nat. Clim. Change* **7**, 817. (doi:10.1038/nclimate3421)
41. Sierra CA, Trumbore SE, Davidson EA, Vicca S, Janssens I. 2015 Sensitivity of decomposition rates of soil organic matter with respect to simultaneous changes in temperature and moisture. *J. Adv. Model. Earth Syst.* **7**, 335–356. (doi:10.1002/2014MS000358)
42. Teuling AJ *et al.* 2010 Contrasting response of European forest and grassland energy exchange to heatwaves. *Nat. Geosci.* **3**, 722. (doi:10.1038/ngeo950)
43. Konings AG, Gentine P. 2017 Global variations in ecosystem-scale isohydricity. *Glob. Change Biol.* **23**, 891–905. (doi:10.1111/gcb.13389)
44. Martínez-Vilalta J, Garcia-Forner N. 2017 Water potential regulation, stomatal behaviour and hydraulic transport under drought: deconstructing the iso/anisohydric concept. *Plant Cell Environ.* **40**, 962–976. (doi:10.1111/pce.12846)
45. Sippel S, Reichstein M, Ma X, Mahecha MD, Lange H, Flach M, Frank D. 2018 Drought, heat, and the carbon cycle: a review. *Curr. Clim. Change Rep.* **4**, 266–286. (doi:10.1007/s40641-018-0103-4)
46. Jentsch A *et al.* 2011 Climate extremes initiate ecosystem-regulating functions while maintaining productivity. *J. Ecol.* **99**, 689–702. (doi:10.1111/j.1365-2745.2011.01817.x)
47. Lu M, Zhou X, Yang Q, Li H, Luo Y, Fang C, Chen J, Yang X, Li B. 2013 Responses of ecosystem carbon cycle to experimental warming: a meta-analysis. *Ecology* **94**, 726–738. (doi:10.1890/12-0279.1)
48. June T, Evans JR, Farquhar GD. 2004 A simple new equation for the reversible temperature dependence of photosynthetic electron transport: a study on soybean leaf. *Funct. Plant Biol.* **31**, 275–283. (doi:10.1071/FP03250)
49. Von Caemmerer S. 2000 *Biochemical models of leaf photosynthesis*. Techniques in Plant Science, no. 2. Collingwood, Australia: CSIRO Publishing.
50. Wu J *et al.* 2017 Partitioning controls on Amazon forest photosynthesis between environmental and biotic factors at hourly to interannual timescales. *Glob. Change Biol.* **23**, 1240–1257. (doi:10.1111/gcb.13509)
51. Quan Q, Tian D, Luo Y, Zhang F, Crowther TW, Zhu K, Chen HY, Zhou Q, Niu S. 2019 Water scaling of ecosystem carbon cycle feedback to climate warming. *Sci. Adv.* **5**, eaav1131. (doi:10.1126/sciadv.aav1131)
52. Poulter B *et al.* 2014 Contribution of semi-arid ecosystems to interannual variability of the global carbon cycle. *Nature* **509**, 600. (doi:10.1038/nature13376)
53. Tang G, Arnone III J, Verburg P, Jasoni R, Sun L. 2015 Trends and climatic sensitivities of vegetation phenology in semiarid and arid ecosystems in the US Great Basin during 1982–2011. *Biogeosciences* **12**, 6985–6997. (doi:10.5194/bg-12-6985-2015)
54. Chapin III FS, Matson PA, Vitousek P. 2011 *Principles of terrestrial ecosystem ecology*. Berlin, Germany: Springer Science & Business Media.
55. Lobell DB, Roberts MJ, Schlenker W, Braun N, Little BB, Rejesus RM, Hammer GL. 2014 Greater sensitivity to drought accompanies maize yield increase in the US Midwest. *Science* **344**, 516–519. (doi:10.1126/science.1251423)
56. Zhang Y, Xiao X, Zhou S, Ciais P, McCarthy H, Luo Y. 2016 Canopy and physiological controls of GPP during drought and heat wave. *Geophys. Res. Lett.* **43**, 3325–3333. (doi:10.1002/2016gl068501)
57. Richardson AD, Hollinger DY, Aber JD, Ollinger SV, Braswell BH. 2007 Environmental variation is directly responsible for short- but not long-term variation in forest-atmosphere carbon exchange. *Glob. Change Biol.* **13**, 788–803. (doi:10.1111/j.1365-2486.2007.01330.x)